# Modeling and Characterization of Thin Film Broadband Resistors on LCP for RF Applications

Stephen Horst*, Swapan Bhattacharya, Seth Johnston, Manos Tentzeris, and John Papapolymerou
School of Electrical and Computer Engineering
Georgia Institute of Technology
85 Fifth Street NW, Atlanta, GA 30308
*shorst@gatech.edu, Phone (678) 592-7911

**Abstract**

Resistors have several applications in high frequency circuits including uses in attenuators, terminations, and power dividers among others. To date, there has been very little attempt to characterize embedded resistor performance on organics above 18 GHz. In this paper, RF measurements of embedded thin film resistors up to 40 GHz are presented on a liquid crystal polymer (LCP) substrate using a commercially available laminated foil to form the thin film NiCrAlSi resistors. Measurements have been demonstrated to be accurate to 5% of their simulated values across the frequency band.

**Introduction**

Over the past few years, Liquid Crystal Polymer (LCP) substrates have emerged as a promising material for achieving fully integrated system on package solutions at RF and millimeter wave frequencies. In order to make that vision a reality, there must be a cost effective and repeatable method of creating embedded passives including the broadband resistors required by a variety of RF circuits. Previous processes for creating these integrated RF resistive loads have involved a highly controlled deposition of a thin film resistive material such as NiCr or TaN onto the substrate [1]. However, direct deposition onto the substrate can be expensive since even small variations in the thickness of the thin film can result in unacceptable variations in sheet resistance. This paper offers results for a different method in which a sheet of copper foil with an integrated NiCrAlSi resistive layer is laminated to the substrate. Integrating the thin film onto rolls of copper foil can reduce costs by outsourcing the critical deposition step to a third party company for dedicated large scale production. The foil transfer process described here is already widely used in printed circuit boards [2, 3]. We intend to demonstrate that it can also be effective for higher frequency circuits up to 40 GHz.

Loads ranging from 0 to 500 Ohms can be fabricated using this technique based on currently available sheet resistance values. Resistors can then be fabricated by means of a two-step wet etching procedure using commonly available chemicals. This process is compatible with large format printed circuit board fabrication at a lower cost. A nickel alloy was used for this application because of its small parasitics and low temperature coefficient of resistance in the range -20 to 100 ppm/$^{o}$C [4].

**Fabrication**

The integrated foil used for this process is ½ oz. copper with NiCrAlSi sputtered onto the matte side using a roll-to-roll vacuum deposition technique. The thickness of the film ranges from 100 to approximately 400 Angstroms depending on the desired sheet resistance. These films are commercially available with various sheet resistances ranging from 25 to 250 Ω/sq. Thinner ¼ oz. copper foils can also be used for finer feature sizes. Measurements with a four-point probe have shown that the sheet resistance of the foils varies within approximately 5% of its stated value. The foil is laminated to 4 mil thick LCP ($\varepsilon_r$=3.16, tan δ=0.003 @ 40 GHz) using a heat press. Lamination has been demonstrated both with and without the use of a low-temperature bond ply adhesion layer which is generally adopted for bonding to substrates.

The remainder of the fabrication process is a two-step wet etching procedure using patterned photoresist masks as demonstrated in Figure 1. The first etching step is used to etch through both the copper and resistive layers to pattern the physical shape of the structures. The second etch exposes the resistors by selectively removing the copper layer.

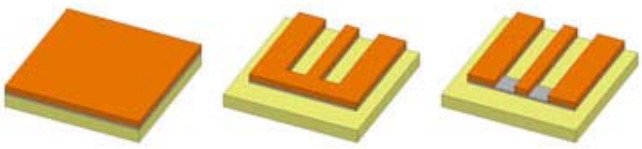

A. Lamination B. First Etch C. Second Etch

Figure 1. Resistor fabrication process

A variety of resistive RF terminations were fabricated using a basic coplanar waveguide topology. As can be seen in Figure 2, this structure consists of exposed resistive strips to bridge the gaps between the center conductor and the ground lines. These were fabricated both with and without a ground plane backing.

When using a conductor backed CPW structure, care must be taken not to excite any spurious modes. In addition to parallel plate modes arising when the width of the structure is greater than $\lambda_{eff}/2$, microstrip modes are also possible when the width of the CPW gaps approaches the same order as the substrate thickness. At the same time, CPW gaps that are too narrow will make etching accurate resistors more difficult. On a standard 4 mil thick LCP substrate, conductor backed CPW gaps should not exceed 100 μm to avoid exciting these spurious modes.

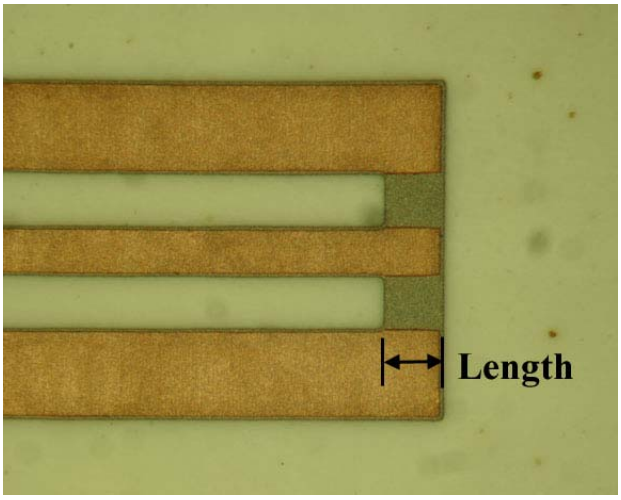


Figure 2. RF terminations

Due to the small size of the resistors, a length of transmission line was added to the terminations to allow the CPW fields to set up properly after transitioning from the probes. Extending from the length dimension in Figure 2, these lines were de-embedded from the measurements as part of a TRL calibration.

**Termination Model**

A back of the envelope derivation for modeling this topology begins with the circuit model for a distributed transmission line seen in Figure 3. When a propagating quasi-TEM CPW wave is incident on the termination, the thin film resistive material will increase the conductance term, G, through each "arm" from center conductor to ground plane as well as add some series inductance inherent to the material. If we ignore conductor losses through the copper, the R term can be ignored. And because the terminations are electrically small, the per unit length L and C can be approximated as a standard inductor and capacitor. This leaves the circuit model seen in Figure 4.

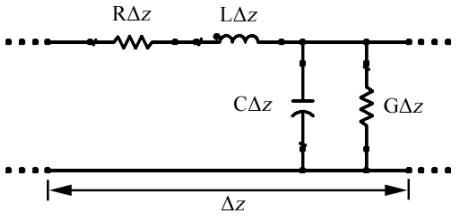


Figure 3. Distributed transmission line model

The value of the resistances $R_1$ and $R_2$ can be calculated by multiplying the sheet resistance of the foil with the length to width ratio of each thin film resistor. This is an ideal calculation that does not include non-idealities, which will be discussed later. Estimates for L and C can be determined using the CPW circuit derivation method outlined in [5]. An additional amount of parallel plate capacitance will need to be added if the CPW structure has a conductor backing. The series inductance values $L_{S1}$ and $L_{S2}$ were extracted from sample resistor measurements. This inductance is inherent to the currents looping through the thin film resistors as seen in Figure 5. The value of the inductance will vary with the size of the loop; however since the width of the CPW gap does not vary much, the diameter of the loop stays fairly constant for each of the termination sizes tested. Therefore the values of $L_{S1}$ and $L_{S2}$ can be approximated as 26pH for CPW gaps on the order of 100um wide.

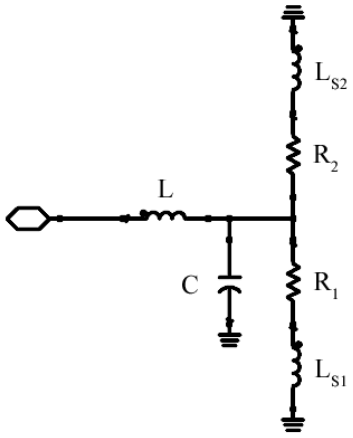


Figure 4. Termination model

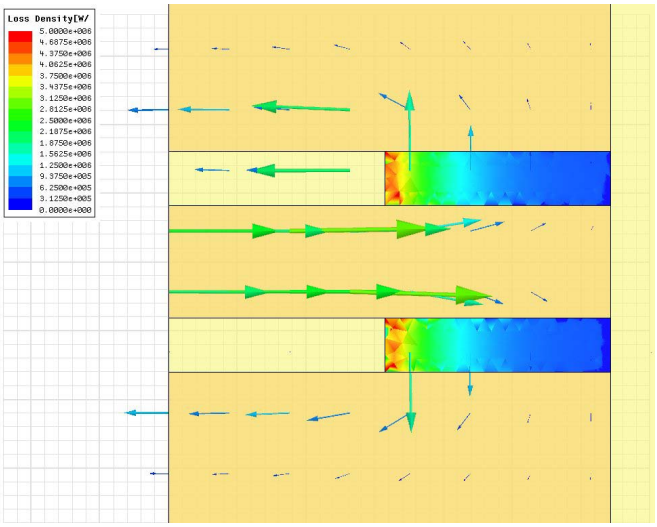


Figure 5. Current vector and loss density in a long termination

Much more accurate simulations can be obtained using full wave analysis software. These simulations can be done quickly by defining the CPW lines as perfect conductors and the thin film resistors as impedance boundaries with the appropriate sheet resistance. Most simulation packages will also require a small de-embedded length of line to be attached to the termination as well in order to properly solve the port fields. The model geometry is simple enough that simulations accounting for conductor thickness and loss can be done in a reasonable amount of time. The simulation can be cut in half down the middle of the center conductor with a magnetic boundary to reduce simulation time if so desired.

**Non-ideality Approximations**

The model presented thus far has ignored non-idealities such as conductor losses. These losses can shift the resistance of the termination by several percentage points, especially when using longer resistors on low sheet resistance foils. There are three primary mechanisms that alter the model:

- Standard transmission line losses (conductor losses, dielectric losses, and radiation losses)
- Skin effect
- Non-uniform lateral currents

Equations for the transmission line losses of a CPW line are well characterized [6]. The conductor losses can be added to the model as a series resistance on the port. This will make up the most significant source of loss and is given as

$$\alpha_c = \frac{R_S \sqrt{\varepsilon_{r,eff}}}{480\pi \cdot K(k)K(k')k'}\left[\Phi(w)+\Phi(d)\right] \text{ (Np/m)} \qquad (1)$$

where $w$ is the width of the center conductor, $d$ is the horizontal distance between the CPW ground planes, $k$ is $d/w$, $k'$ is the complement $\sqrt{1-k^2}$, $K(k)$ is the elliptic integral of the first kind, $R_S$ is the surface resistivity of copper, and $\Phi(x)$ is given as

$$\Phi(x) = \frac{\pi}{x} + \frac{1}{x}\ln\left[\frac{8\pi x(1-k)}{t(1+k)}\right] \qquad (2)$$

$t$ is the thickness of the conductor. Dielectric losses can be represented as a conductance in parallel with the capacitance from Figure 4.

$$\alpha_d = \frac{q\varepsilon_r \tan(\delta_e)}{\varepsilon_{eff}\lambda_g} \text{ (Np/m)} \qquad (3)$$

Radiation losses are small compared to the conductor and dielectric losses and are considered to be negligible in terms of the circuit model. Equivalent equations for conductor backed CPW can be found in [7].

The resistor model from Figure 4 and conductor losses calculated in (1) assume that the current flows uniformly through the conductor. The skin effect will increase this loss by decreasing the area of current flow. As the frequency increases the currents will tend to the surface of the conductor where they will fall off exponentially based on the skin depth. The skin depth is a frequency dependent parameter given by

$$\delta_S = \sqrt{\frac{\rho}{\pi f \mu_0 \mu_r}} \qquad (4)$$

The resistivity, $\rho$, of the resistor foils can be calculated from the sheet resistance and the thickness of the thin film. Assuming a relative permeability of 100 caused by the ferromagnetic properties of nickel, the skin depth in the thin film at the highest measured frequency is approximately 800 Å. Because the thin film ranges from 100 to 400 Å in thickness, the currents should be able to flow through the resistors uniformly, indicating that the skin effect will have little influence on the resistors up to 40 GHz. The thick copper conductors are another matter. The skin depth in copper is about 325 Å at 40 GHz. Since the copper is 18 um thick the conductor losses will be frequency dependent as the area of current flow decreases. The surface roughness of the copper will also add to the conductor losses as the frequency increases. A study of this effect is given [8].

Figure 6 shows the combined conductor and dielectric losses when accounting for the skin effect. In order to accurately model the measured transmission line, the loss through the underlying thin film must also be considered. One side effect of the lamination process is that the lossy thin film will exist underneath all of the patterned copper structures on that layer. Since nickel composites are often used for adhesion seed layers this will aid in the bond strength of the foil to the LCP, but it will also intensify the conductor loss as the skin effect forces the currents to the surface. This effect can be modeled by integrating the exponential decay of the currents along the thickness of the conductor with respect to the skin depth. Approximately 63% of the current will be contained within one skin depth so as the skin depth decreases more current will go through the underlying thin film.

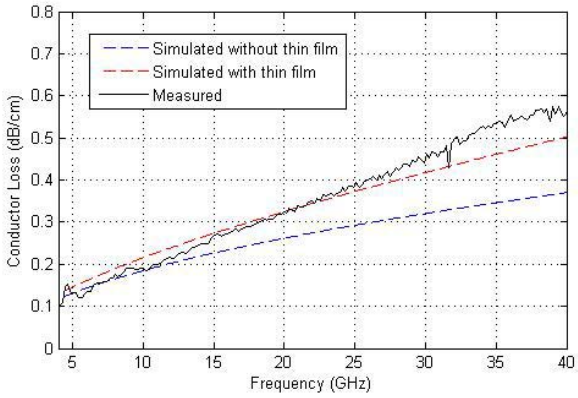


Figure 6. Modeling transmission line losses with the skin effect

Non-uniform lateral currents produce similar results to the skin effect. This effect is best visualized by the loss density plot in Figure 5. In the mesh plot, areas of high loss per unit area are red while areas of low loss are blue. This figure shows that the losses, and therefore the currents, are mostly concentrated toward the front of the termination. The effect is most prominent on long terminations using low sheet resistance foils. The termination shown is four squares long and uses a 25 Ω/sq thin film. This effect can have a significant impact on the performance of the termination, and is best modeled using a simulation package.

**Measurements**

Measurements were taken on long terminations with low sheet resistance foils for comparison to simulations. These terminations were considered the most difficult to simulate because they contain the most parasitics and lateral current effects. Figure 7 shows the impedance measurements of a termination with a length of four squares and a sheet resistance of 25 Ω/sq.

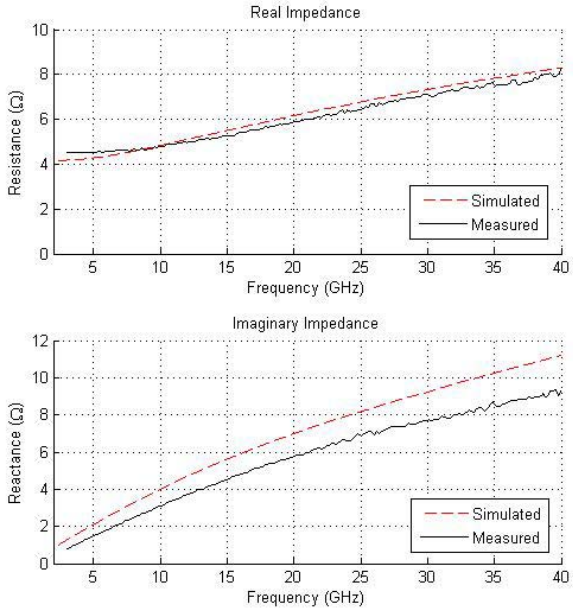


Figure 7. Long resistor impedance measurement

These results show that the simulations match up quite well with the actual measurements. The only significant deviation is that the simulation slightly over estimates the reactance in the termination.

Very short terminations were also measured to avoid the parasitic effects described previously. When the length of the termination is sufficiently small, the reactive components become small enough to be negligible, approximating only the ideal resistors in parallel. For these measurements a 25 Ω/sq foil was used and resistors were fabricated at various sizes down to ¼ squares in length. This is equivalent to 50 um based on the width of the CPW. A sample resistor with a length of approximately 0.5 squares is shown in Figure 8. The dashed line represents the simulated value of the resistor. The termination stays well within a 5% variation of its simulated value throughout the full 2 to 40 GHz band. In Figure 9, a Smith chart representation of the same sample reveals the imaginary component of the termination is very small as well, since the measurement is concentrated on the real axis.

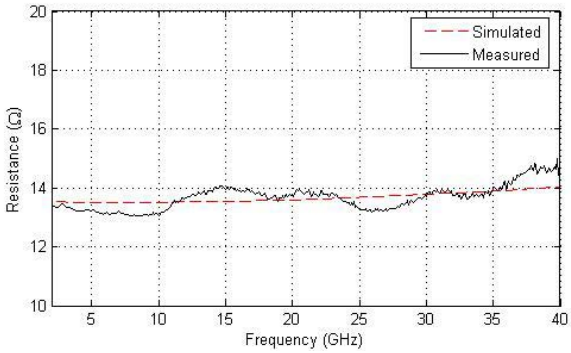


Figure 8. Short resistor impedance measurement

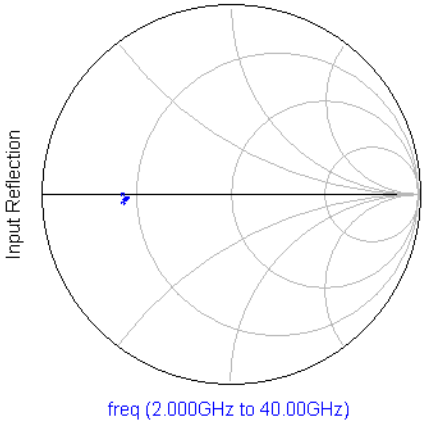


Figure 9. Termination reflection coefficient to 40 GHz

Figure 10 shows a number of resistance measurements compared to their ideal values. The measured and modeled values compare nicely until the termination length becomes shorter than half of a square, which corresponds to approximately 100 µm. As the length of the terminations decreases, its resistance will increase on an order inverse to the length of the termination. Eventually this increasing slope will cause measurement inaccuracies due to the feature size limitations on ½ oz. copper.

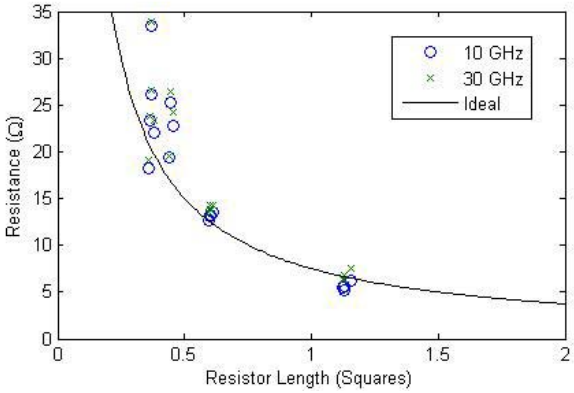


Figure 10. Termination Measurements Across Size

## Conclusions

Laminated foil resistor measurements up to 40 GHz on low loss LCP substrates have been presented for the first time to the best of our knowledge. A model has been presented that provides the circuit performance for terminations of arbitrary length. The lamination process for integrated resistors has the potential to reduce the cost of creating accurate resistances across a wide band of frequencies. The terminations measured here were accurate to 5% based on their measured physical dimensions.


## Acknowledgments

The authors would like to thank Rogers Corporation for supplying the LCP and Gould Electronics for supplying the resistor foils. Thanks also to our sponsors: the Georgia Electronic Design Center and the Package Research Center.


## References


1. R. Sharma, S. Vinayak, et al., "RF Parameter Extraction of MMIC Nichrome Resistors," *Microwave and Optical Technology Letters*, vol. 39, no. 5, Dec. 2003, p. 409-412
2. L.J. Salanzo, C. Wilkinson, and P.A. Sanborn, "Environmental qualification testing and failure analysis of embedded resistors," *IEEE Trans. on Advanced Packaging*, vol. 28, no. 3, Aug. 2005, p. 503-20
3. L. D'Souza, "Embedded Passives, RF Design," *Advanced Packaging*, vol. 13, no. 11, Nov. 2004, p. 34-38
4. "TCR, TCR+ copper foil with integrated thin film resistor datasheet," Internet: http://www.gouldelectronics.com/download/tcr.pdf, February 2, 2006
5. W. Heinrich, "Quasi-TEM description of MMIC coplanar lines including conductor-loss effects," *IEEE Trans. on Microwave Theory and Techniques*, vol. 41, no. 1, Jan. 1993, p. 45-52
6. B.C. Wadell, Transmission Line Design Handbook, Artech House (Boston, 1991), p. 73-76
7. F. Schneider, T. Tischler, and W. Heinrich, "Modeling dispersion and radiation characteristics of conductor-backed CPW with finite ground width," *IEEE Trans. On Microwave Theory and Techniques*, vol. 51, no. 1, Jan. 2003, p. 137-43
8. G. Brist, S. Hall, et al., "Non-classical conductor losses due to copper foil roughness and treatment," Internet: http://www.gouldelectronics.com/papers/CopperSurfaceLoss.pdf
9. J. Kraus and D. Fleisch, Electromagnetics with Applications, 5th ed. McGraw-Hill (Boston, 1999)
10. B. Lee, G. Park, J. Kim, and D. Lee, "The effect of the process parameters on the electrical properties of Ni-Cr-Si alloy thin resistor films," *Conf. on Electrical Insulation and Dielectric Phenomena*, p. 72-74, 2002
11. Z.D. Schwartz, G.E. Ponchak, et al., "Measurement of Thin Film Integrated Passive Devices on SiC through 500C," *Conf. Proc. 34th European Microwave Conference*, vol. 1, pt. 1, p. 313-316, 2004